

Supplementary Information

Electroless deposition of Ni-P/Au coating on Cu substrate with improved corrosion resistance from Au(III)-DMH based cyanide-free plating bath using hypophosphite as a reducing agent

Bo Wu,^a Baizhao Tan,^a Guizhen Tan,^a Ming Zeng,^a Jinyi Luo,^a Guanghui Hu,^a Jiye Luo,^a Zhifeng Hao,^{*a} Shaomei Lai^b and Binyun Liu^{*b}

^a *Guangdong Provincial Key Laboratory of Plant Resources Biorefinery, School of Chemical Engineering and Light Industry, Guangdong University of Technology, Guangzhou 510006, China*

^b *Guangdong Toneset Science & Technology Co., Ltd., Guangzhou 511400, China*

* Correspondence to: haozf@gdut.edu.cn (Zhifeng Hao)
beston@ghotech.com (Binyun Liu)

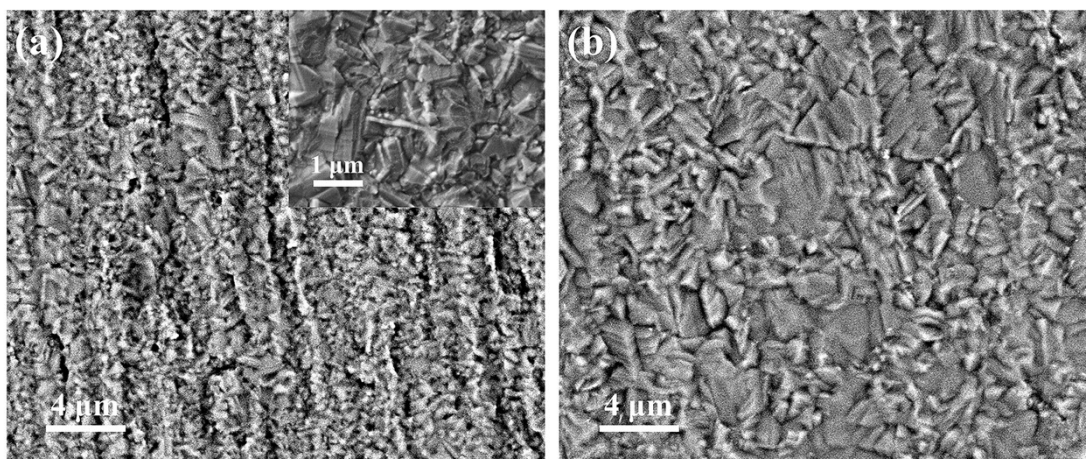


Fig. S1 SEM images of the copper sheets: (a) without pretreatment and (b) after soaking in a mixed solution of 5 wt.% sulfuric acid and $60 \text{ g L}^{-1} \text{ Na}_2\text{S}_2\text{O}_8$

It can be seen from Fig. S1 that the copper particles without pretreatment are tiny. After the treatment of the mixed solution consisting of 5 wt.% sulfuric acid and $60 \text{ g L}^{-1} \text{ Na}_2\text{S}_2\text{O}_8$, the copper surface becomes rough. This rough structure will help to improve the adhesion between Cu substrate and Ni-P layer.

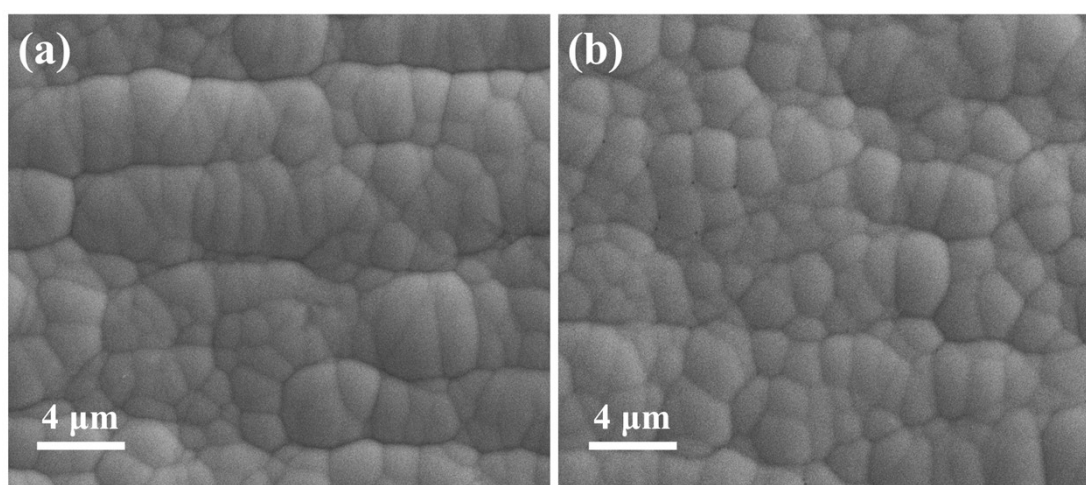


Fig. S2 SEM images of the Ni-P layers (a) before and (b) after the stripping process

Table S1 Reaction time for depositing 0.05 μm Au layer in plating bath containing different concentrations of NaH_2PO_2

NaH_2PO_2 concentration / g L^{-1}	Reaction time / min
0	15
2.5	13
5.0	11
7.5	9
10.0	8

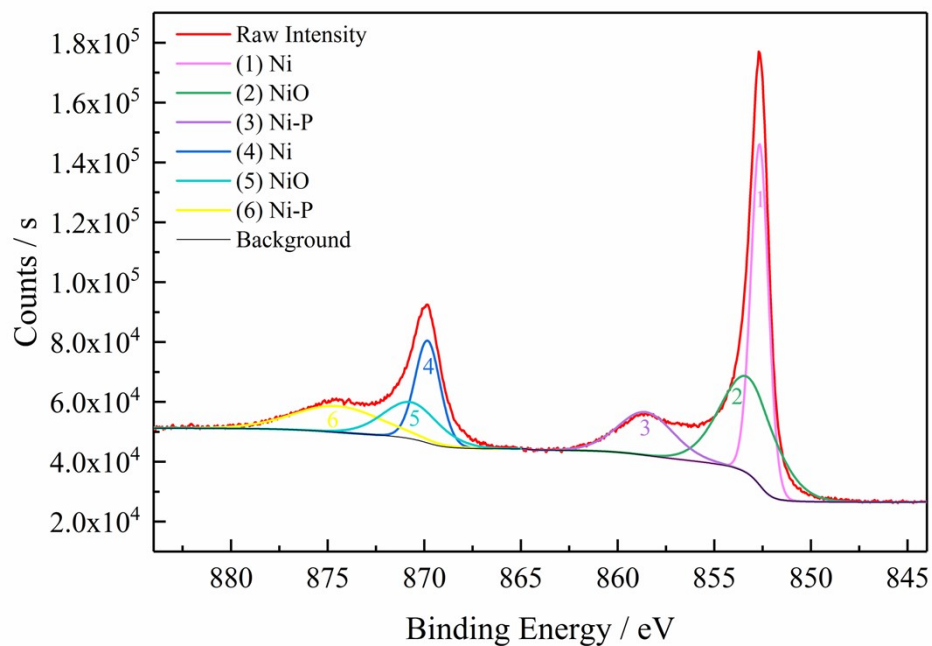


Fig. S3 Fitted high-resolution Ni 2p spectrum after etch 150 nm.

Table S2 Elemental contents of Au, Ni, P, and O obtained from depth profiles

Etch depth / nm	Au / at.%	Ni / at.%	P / at.%	O / at.%
10	100	0	0	0
20	100	0	0	0
30	100	0	0	0
40	100	0	0	0
50	93.71	5.71	0.59	0
60	71.28	22.34	5.90	0.48
70	44.28	45.56	9.49	0.67
80	26.85	59.47	11.93	1.75
90	17.07	68.09	12.48	2.36
100	11.89	72.17	13.24	2.71
110	8.56	74.56	12.59	3.29
120	6.52	77.02	12.53	3.93
130	4.95	78.82	12.12	4.11
140	4.24	79.11	12.33	4.32
150	3.81	79.97	12.24	4.23

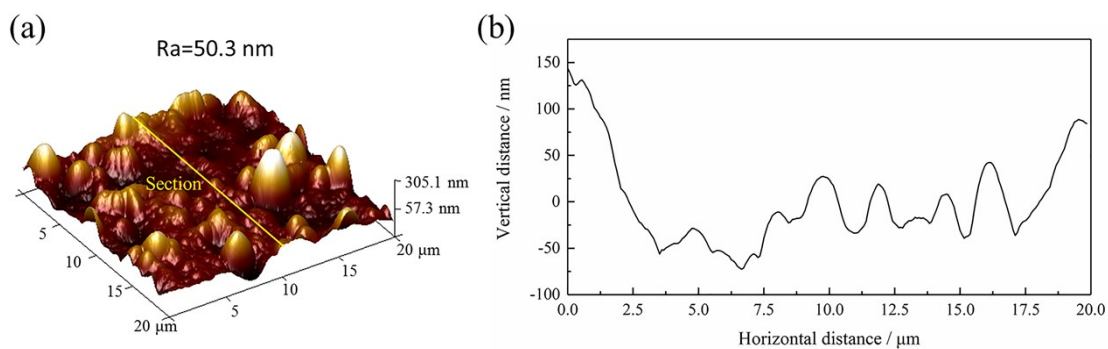


Fig. S4 (a) AFM image of the Ni-P layer and (b) the sectional analysis of AFM image.

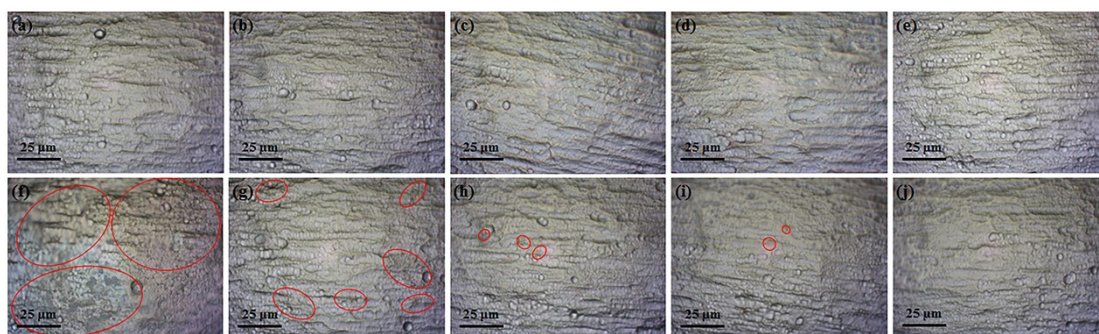


Fig. S5 Optical microscope images of the Au layers before (a-e) and after (f-j) salt spray tests. The Au layers were deposited from cyanide-free bath containing different concentration of NaH_2PO_2 : (a, f) 0 g L^{-1} , (b, g) 2.5 g L^{-1} , (c, h) 5.0 g L^{-1} , (d, i) 7.5 g L^{-1} , and (e, j) 10 g L^{-1} .

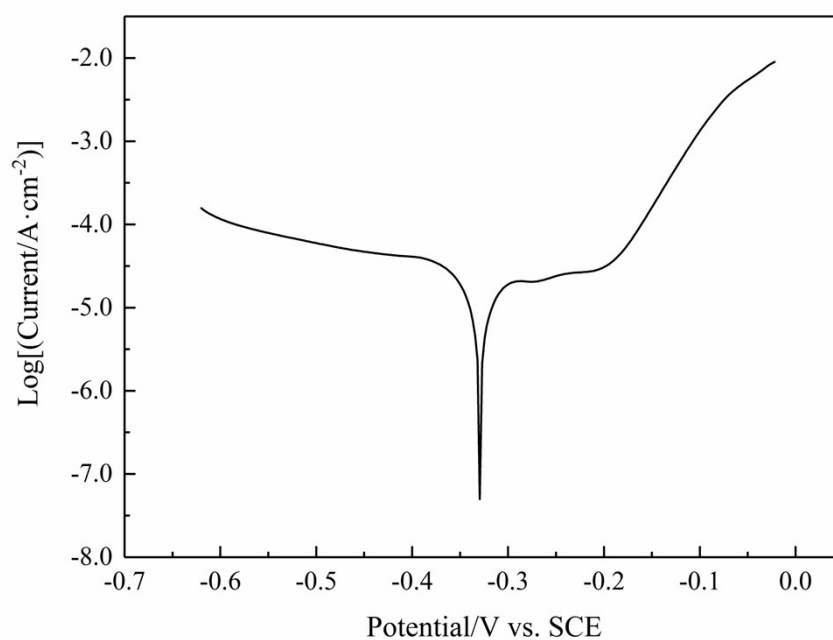


Fig. S6 The PDP curve of Cu substrate in a 3.5 wt.% NaCl solution.

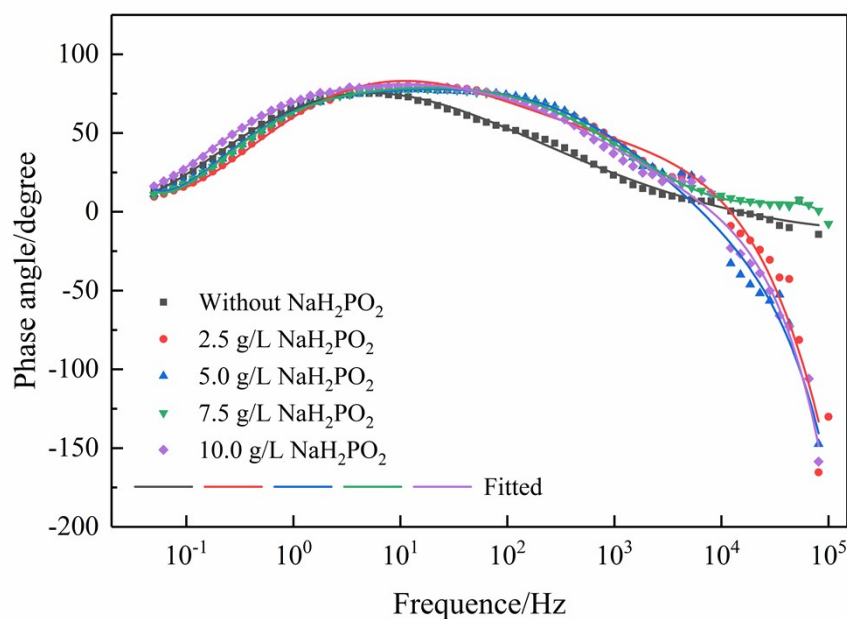


Fig. S7 Bode phase plots of the coatings in a 3.5 wt.% NaCl solution.

Table S3 Electrochemical parameters for EIS tests in a 3.5 wt.% NaCl solution

Concentration of NaH_2PO_2 (g L^{-1})	R_s ($\Omega \text{ cm}^{-2}$)	R_{coat} ($\Omega \text{ cm}^{-2}$)	CPE_{coat}		CPE_{dl}	
			Y_0 ($\mu\text{F cm}^{-2}$)	n	Y_0 ($\mu\text{F cm}^{-2}$)	n
0	6.21	22.44	12.29	0.897	18.42	0.876
2.5	5.53	60.27	8.77	0.932	3.15	0.891
5.0	6.66	112.7	7.39	0.966	6.81	0.784
7.5	6.51	80.85	10.92	0.911	1.75	0.825
10.0	6.22	310.17	15.38	0.927	2.35	0.792

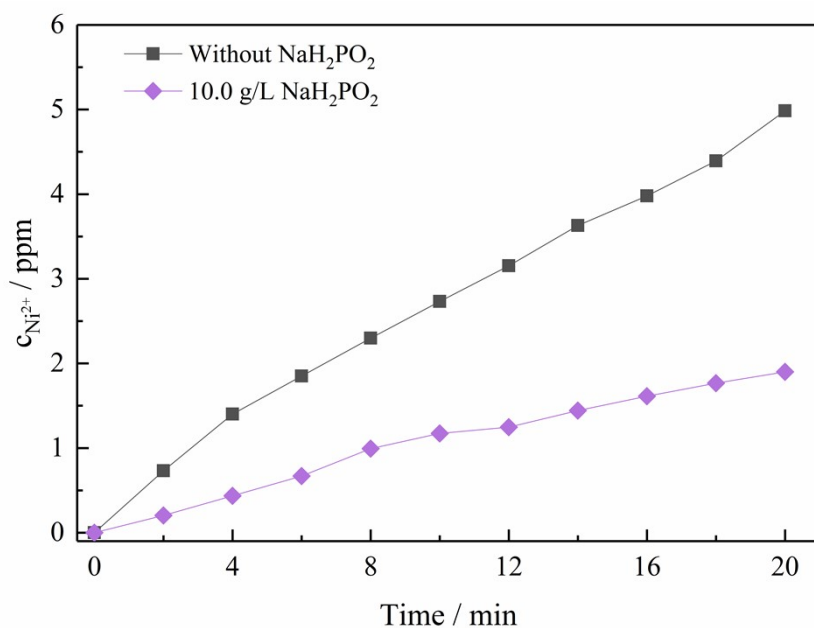


Fig. S8 The concentrations of the generated nickel ions vary with the reaction time.

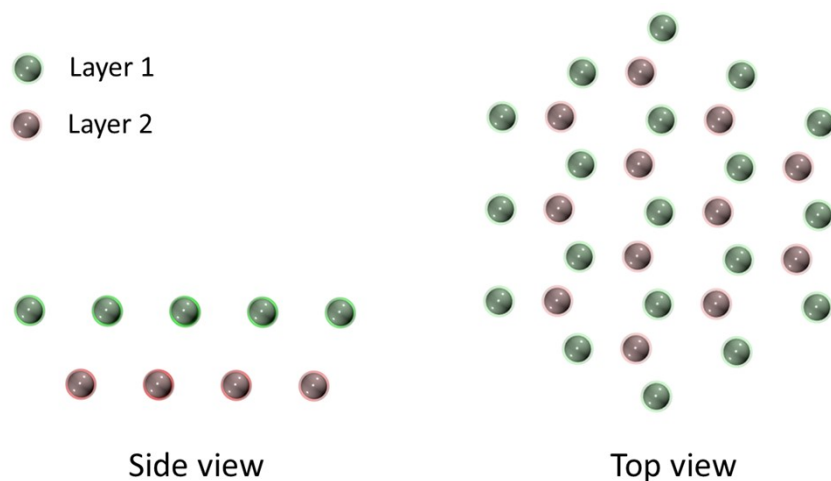


Fig. S9 Side view and top view of the cluster.

Cluster models were often used to simulate metal surfaces.¹⁻⁶ XRD analysis has revealed that the Au(111) was the preferential orientation, so the (111) facet was constructed.

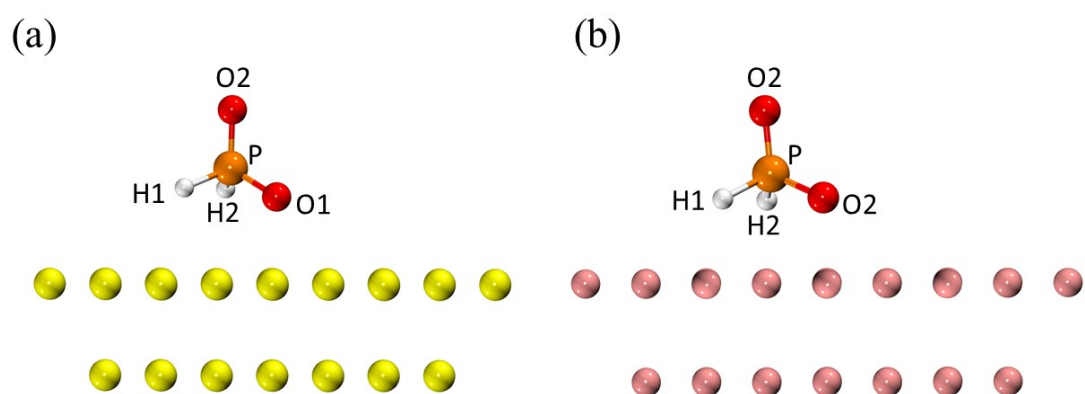


Fig. S10 Side view for the structures of hypophosphite adsorbed on Au₃₁ cluster (a) and Cu₃₁ cluster (b). White: H, orange: P, yellow: Au, pink: Cu.

Table S4 Bond length and bond angle parameters of hypophosphite adsorbed on Au₃₁ and Cu₃₁ cluster

Parameters	H ₂ PO ₂ ⁻ -Au ₃₁	H ₂ PO ₂ ⁻ -Cu ₃₁
<i>r</i> (P-O1)/Å	1.554	1.541
<i>r</i> (P-O2)/Å	1.508	1.510
<i>r</i> (P-H1)/Å	1.438	1.453
<i>r</i> (P-H2)/Å	1.439	1.455
θ (O1-P-O2)/°	116.988	118.539
θ (H1-P-O2)/°	112.034	111.581
θ (H2-P-O2)/°	111.996	111.233
θ (O1-P-H2)/°	106.873	107.116
θ (O1-P-H1)/°	106.939	106.989
θ (H1-P-H2)/°	100.593	99.603

References

- 1 T. Homma, I. Komatsu, A. Tamaki, H. Nakai and T. Osaka, *Electrochim. Acta*, 2001, **47**, 47-53.
- 2 T. Shimada, K. Sakata, T. Homma, H. Nakai and T. Osaka, *Electrochim. Acta*, 2005, **51**, 906-915.
- 3 M. Kunimoto, T. Shimada, S. Odagiri, H. Nakai and T. Homma, *J. Electrochem. Soc.*, 2011, **158**, D585.
- 4 M. Kunimoto, K. Seki, H. Nakai and T. Homma, *Electrochemistry*, 2012, **80**, 222-225.
- 5 M. Kunimoto, K. Endo, H. Nakai and T. Homma, *Electrochim. Acta*, 2013, **100**, 311-316.
- 6 S.S. Starodubov, I.V. Nechaev and A.V. Vvedenskii, *Russ. J. Phys. Chem. A*, 2016, **90**, 122-129.